LINJ1J'ATIONS ON THE SUBCARRIER FREQUENCY-TO-SYMBOL RATE RATIO

Loc V. lam, Tien M. Nguyen, Sami M. Hinedi, Biren Shah, Aseel Anabtawi

A-E-93-26

National Aeronautics And Space Administration
Jet Propulsion Laboratory
California Institute of Technology
4800 Oak Grove Drive
Pasadena, California 91109

ABSTRACT

For space missions in which tracking the residual carrier is absolutely critical, the use of a subcarrier to separate the data from the residual carrier is the best way to maximize residual-carrier tracking performance. In exchange for a better tracking performance, this method consumes greater bandwidth than required without a subcarrier. In this paper, the residual-carrier tracking performance for PCM/PSK/PM/NRZ for square wave and sine wave subcarriers will be determined as a function of the subcarrier-to-sy mbol rate ratio. Explicitly, the RF residual carrier hacking performance in terms of the symbol SNR degradation will be quantified. The upper and lower bound values for the subcarrier-to-symbol rate ratio will also be derived, and for which they can be used to determine the minimum required bandwidth for maximum residual-carrier tracking performance. The analytical results obtained from the mathematical models are validated by computer simulation

I. INTRODUCTION

Currently, most space missions operate at relatively low data rates using residual carrier modulation, thus necessitating the separation of the data from the residual carrier to avoid interference. This can be achieved by placing the data modulation on a subcarrier, since direct modulation of the data on the carrier would cause most of the data power to fall within the bandwidth of the carrier Phase-1 .ocked-I mop (PLL) and, as a consequence, interfers with its operation [1, chap. 3]. The scheme in which the data is Phase-Shift Keyed (PSK) onto a subcarrier and then l'base-hlodLllated (PM) onto a sinusoidal carrier is called PCM/PSK/PM modulation scheme. Furthermore, the international Consultative Committee for Space Data Systems (CCSDS) has recommended that the square wave subcarrier should be used for the deep space missions and sine wave subcarrier for the near earth missions [3].

The performance evaluation of the PCM/PSK/PM for both square wave and sine wave subcarriers has been evaluated and became text book material [1, 4 and 7]. However, the analyses presented in [], 4 and 7] have always assumed that the subcarrier frequency-to-symbol rate, n, is sufficiently high enough that the interaction between the RF residual carrier and data is negligible. Recently, [2] has calculated the minimum allowable n for PCM/PSK/PM with high symbol rate and square wave subcarriers only.

The purpose of this paper is to determine the minimum (lower bound) n and to present a simplified approximate-mathematical model to evaluate the upper bound of n for PCM/PSK/PM with both square wave and sine wave subcarriers. Using the available results [1 -7], this paper will quantify the lower bound of n in terms of the Symbol Signal-to-Noise Ratio (SSNR) degradation and the upper bound of n in terms of power Containment in the predetection filter bandwidth. The paper is organized as follows: A brief description of the residual carrier modulation scheme

with associated Power Spectral Density (PSD) is presented in Section 2. The performance of the PCM/PSK/PM system as a function of n and the derivation of the bounds for n are shown in Section 3 and 4, respectively. A brief description of the computer simulation to verify the theory derived in Sections 3 and 4 is presented in Section 5. Numerical results are shown in Section 6 and genera] discussions and conclusions arc presented in Section 7.

II. TELEMETRY FORMAT

Telemetry format which employs PCM/PSK/PM modulation scheme with either a sine wave or a square wave subcarrier can be represented mathematically as [1, 4 and 7]

$$S_T(t) = \sqrt{2P_T}\cos(\omega_c t + md(t)p(t)) \tag{1}$$

where P_T is the total transmitted power, m is the modulation index, d(t) is the non-return-to-zero data format (NRZ), and p(t) is either a sine wave or a square wave subcarrier as shown in Eqns. (1a) and (1 b) respectively,

$$p(t) = \begin{cases} sqr(\omega_{sc}t + \theta_{sc}) & (1a) \\ \sin(\omega_{sc}t + \theta_{sc}) & (1b) \end{cases}$$

For p(t) = sqr(.), one has PCM/PSK/PM/Square-wave. Using simple trigonometric expansions, Eqns (1) and (1a) can be expressed as a sum of the residual carrier component and the data component. Explicitly,

$$s_{T,SQUARE}(t) = \sqrt{2P_T}\left\{\cos(m)\sin(\omega_c t) + d(t)p(t)\sin(m)\cos(\omega_c t)\right\} \tag{2}$$

where the first term is the carrier component and the second term is the data component. In Eqn. (2), the modulation index, m, allocates the total transmitted power, P_T, between the residual carrier and the data. When p(t) = sin(.), one has PCM/PSK/PM/Sin e-wave, the expansion on

Eqns (1) and (lb) yields

$$s_{T,SINE}(t) = \sqrt{2P_T}\sin(\omega_c t)\left[J_0(m) + \sum_{n=2,\ even}^{\infty} 2J_n(m)\ \mathrm{Cos}\ (\mathrm{Im.et})\right] + \sqrt{2P_T}d(t)\cos(\omega_c t)\left[\sum_{n=1,\ odd}^{\infty} 2J_n(m)\sin(n\omega_{sc}t)\right] \quad (3)$$

where $J_n(m)$ is the Bessel function of the first kind with order n. As before, the modulation index, m, divides the total power, P_T, between the carrier and the data. From Eqn. (2), the power spectral density (PSD) for PCM/PSK/PM /Square-wave subcarrier is found to be [5]

$$s_{,),\ SQUARE}(f) = P_T\left[\cos^2(m)\ \delta(f - f_C) + \frac{4}{\pi^2}\sin^2(m)\sum_{k=1}^{\infty}\frac{1}{(2k-1)^2}\left(S_D(f - f_c - (2k-1)\ f_{sc}) + S_D(f - f_c + (2k-1)\ f_{sc})\right)\right] \quad (4)$$

and the PSD for PCM/PSK/PM/Sine-wave is given by:

$$S_{D,sine}(f) = P_T\left[J_0^2(m)\ \delta(f - f_c) + \sum_{k=1}^{\infty} J_k^2(m)\delta\left((f - f_c - (2k)\ f_{sc}) + \delta(f - f_c + (2k)\ f_{sc})\right) + \sum_{k=1}^{\infty} J_k^2(m)\left(S_D(- f_c - (2k-1)\ f_{sc}) + S_D(f - f_c + (2k-1)\ f_{sc})\right)\right] \quad (5)$$

where $S_D(.)$ is the spectrum density for the NRZ data format which is defined as [1]

$$S_D(f) = \frac{1}{R_s}\cdot\frac{\sin^2(\pi\frac{f}{R_s})}{(\pi\frac{f}{R_s})^2} \quad (6)$$

From Eqn. (4) and (5), the residual carrier power and the data power can be obtained directly as shown respectively for the square wave subcarrier case,

$$P_C = P_T \cos^2(m)$$
$$P_D = P_T \sin^2(m) \qquad (7)$$

and for the sine wave subcarrier case,

$$P_C = P_T J_0^2(\mathrm{m})$$
$$P_D = 2P_T J_1^2(\mathrm{m}) \qquad (8)$$

The PSD functions defined in Eqns. (4), (5) and (6) are plotted in Figs. 1 (a), 1 (b), and (1c) respectively. For clarity sake, only the positive frequency and the first two harmonics are shown in figures 1 (a) and (1b). Equations (4) and (5) are symmetric functions, hence their PSDs for negative and positive frequencies are mirror of each other,

111, PERFORMANCE ANA] .YSIS

At the ground station receiver, a PLL is employed to track the residual carrier in the incoming signal. The performance of the 1'1,1, depends on how much data power is present inside the carrier tracking loop bandwidth which interfers with the carrier. The amount of interference from the data depends on the subcarrier frequency-to-symbol rate ratio, n. The shaded region in Fig. 1 illustrated this effects. interference of this type causes the PLL to provide imperfect reference to the tracking of residual earl-icr, which can be modelled mathematically as

$$C(n, t) = \sqrt{2P_T}\cos(\omega_c t + \phi(n,t)) \qquad (9)$$

where $\phi(n,t)$ denotes the carrier tracking phase errors induced by the data interference, and n is the subcarrier-to-sy mbol rate ratio which impacts the phase error. The performance of the latter has been

assessed in the past [1, 2, 4 and 7]. It degrades the Symbol Error Rate (SER) performance. Clearly, as one varies n, or vary the separation between the carrier and the data, one is also varying the performance of residual-carrier tracking. One seeks, therefore, the minimum value of n such that the degradation is minimal. By analyzing the carrier tracking performance and then determining the SER performance one can determine the lower bound n_1. The theory presented in [1 -2] will be used to deter-mine the lower bound n_L. For PCM/PSK/PM/Sine-wave with low data rate and n; higher order harmonics (or spikes) of the carrier can fall within the carrier tracking loop bandwidth and can cause potential CW interference. For this case, analytical results will be verified by computer simulation,

The carrier tracking performance can be characterized by the tracking variance, σ_ϕ^2, which is given by [2]:

$$\sigma_\phi^2 = \frac{1}{\rho_o} ICR \qquad (1.0)$$

where ρ_0 is the ideal PLL loop SNR }t'hit]) is defined in [2] for a square, wave and sine wave subcarriers respectively as

$$\rho_o = \frac{P_T \cos^2(m)}{N_o B_L} \qquad (11)$$

$$\rho_o = \frac{P_T J_o(m)^2}{N_o B_L} \qquad (1.2)$$

and ICR is the interference-power-to-carrier-power ratio and will be derive in the following section.

III.1 EVALUATING ICR

This section derives the ICR parameters for both PCM/PSK/PM/Square-wave and PCM/PSK/PM/Sine-wave cases. The derivation assumes that the interference spectrum is smooth

over the carrier tracking bandwidth, hence it can be characterized as a white noise process. For the case when the interference spectrum is not smooth, computer simulation will be used in analyzing the performance of the system.

111.1.1 SQUAREWAVE CASE.

As the name suggested, ICR is the interference power that falls inside the carrier tracking loop bandwidth to the earl-icr power ratio. Explicitly, for square wave subcarrier case ICR is given by [2]:

$$ICR_{SQUARE} = \tan^2(m) \int_{-B_L}^{B_L} S_{D,SQUARE}(f) |H(f)|^2 df \tag{13}$$

where $S_{D,SQUARE}(f)$ can be found from Eqn. (4), and it is given by:

$$S_{D,SQUARE}(f) = \frac{4}{\pi^2} \sum_{k=1}^{\infty} \frac{S_D(f - (2k-1) f_{sc}) + S_D(f + (2k-1) f_{sc})}{(2k-1)^2} \tag{14}$$

and H(f) is the transfer function of the tracking loop filter given by [1]:

$$|H(f)|^2 = \frac{1 + 2\left(\frac{f}{f_n}\right)^2}{1 + \left(\frac{f}{f_n}\right)^4} \tag{15}$$

where f_n is the natural frequency of the loop filter given by [1]

$$f_n = \frac{B_L}{\pi\left(\xi + \frac{1}{4\xi}\right)} \tag{16}$$

where ζ is the damping factor, and it is assured to be 0.707.

111,1.2 SINEWAVE CASE

For modulation with sine-wave subcarrier, ICR then becomes

$$1CR_{SINE} = \frac{1}{J_0^2(m)} \int_{\infty}^{\infty} S_{D,\,SINE}(f)\,|H(f)|^2 df \qquad (17)$$

where $J_0(m)$ is the Bessel function, $S_{D,SINE}$ is derived from Eqn. (5), and it is given by:

$$S_{D,SINE} = \sum_{k=1}^{\infty} J_{2k-1}^2(m) \left[S_D(f-(2k-1) f_{sc} + S_D(f+(2A-3.) f_{sc}) \right] \qquad (18)$$

and H(f) is defined by Eqn. (15), Eqn. (1'7) is valid as long as $O < B_L < 3f_{sc}$ As illustrated in Fig. (lb), for $B_L > 3f_{sc}$, higher order of the carrier harmonics (see Figure 2.) can fall into the tracking loop bandwidth and can caused (W interference,

1 I I.2 DETERMINING SYMBOL. ERROR I< A'J'}{; (SER)

ideally, when there is no interference and the P] ,loop SNR is infinite, the SER (or Pe) is computed from [1]

$$PC_{IDEAL} = \frac{1}{2} erfc\left(\sqrt{\frac{E_s}{NO}}\right) \qquad (19)$$

where E_S/N_0 is denoted as the symbol SNR and it is given by [1] for the square wave and sine wave subcarriers respectively as

$$\frac{E_s}{N_0} = \frac{P_T}{N_0} \frac{Sin^2(m)}{R_S} \qquad (20)$$

$$\frac{E_S}{NO} = \frac{P_T}{N_o} \frac{2 J_1^2(n))}{R_S} \qquad (21)$$

in practice, the PLL's loop SNR is not infinite (especial 1 y when data interfers with the carrier) and Eqn. (19) becomes

$$Pe = \int_{\phi} erfc\left(\sqrt{\frac{E_s}{N_o}} \cos((j)\right) p(\phi)\, d\phi \tag{22}$$

where ϕ denote the phase error of the VCO in the PLL. The probability density function of the phase error is approximated by a Tikhonov density

$$p(\phi) = 2\pi I_o(\rho), \qquad \phi \in [-\pi, \pi] \tag{23}$$

where ρ is the effective loop SNR which is computed from Eqn. (1 O) to be

$$\rho = \frac{1}{\sigma_\phi^2} = \frac{1}{\rho_o} + ICR \tag{24}$$

Note that Eqn. (22) represents a mathematical model to calculate the Symbol Error Rate (SER) for the case when the data rate is high with respect to the receiver tracking loop bandwidth. For high data rate case, the phase error process $\phi(n,t)$ varies slowly and is essentially constant over a symbol interval $T = 1/R_S$. However, when the data rate is low relative to the receiver tracking loop bandwidth, the phase process is no longer constant over the symbol interval, it varies rather fast over the symbol interval T anti the SER can better be approximated by [1]:

$$Pe \approx \frac{1}{2} erfc\left(\sqrt{\frac{E_s}{N_0}} E[\cos(\phi)]\right) \tag{25}$$

where

$$E[\cos(\phi)] = \int_{\phi} \cos(\phi)\, p(\phi)\, d\phi \tag{26}$$

Once the SER is determined, one can quantify the carrier tracking performance by determining the symbol SNR degradation. For a fixed SER, the symbol SNR degradation can be determined by subtracting the symbol SNR obtained from Eqn. (1 9) for ideal case (i. e., corresponding to $n = f_{SC}/R_S = \infty$ and infinite loop SNR) from the corresponding symbol SNR obtained from Eqn (22) for non-ideal case, (i.e., with data interference and infinite loop SNR.) The difference in the symbol SNR is the degradation due to imperfect residual carrier tracking cause by data interference, Examples will be shown in the numerical results section.

IV. DETERMINING '1'1 IE SUBCARRIER-TO-SYMBOL RATE RA'1'1O BOUNDS

Using the results presented in the last two sections, one can determine the minimum value of the subcarrier-to-symbol rate ratio, n_L, to meet a specific SNR degradation. This can be done by computing the SER using Eqn. (22) or (25) with n as parameter. Unfortunately, as one moves the subcarrier further away from the carrier (increasing n,) one is also pushing the data spectrum out of the bandwidth of the predetection filter as shown in Fig. 2. This filter is usually located in front of the 1'1.1, or at the first IF stage of the receiver and band limits the incoming signal. Hence, with the knowledge of the required minimum data power containment within the predetection filter bandwidth, the maximum allowable value of n can be determined, The total Power Containment (PWC) of the data within the filter bandwidth can be computed from

$$PWC = \int_{-\infty}^{\infty} S(f)\, |H(f)|^2 df \tag{27}$$

where I(f) denotes the transfer function of a bandpass filter and S(f) is the PSD defined in Eqns. (14) and (18) for the square wave and sine wave subcarriers, respectively.

in this paper, the predetection filler assumes the same frequency responds of the filter implemented in the Deep Space Network (DSN)/Block V receiver [1 O]. This filter is a Surface Acoustic Wave (SAW) bandpass filter. The SAW filter has a passband of 66MHz; measured between the -1 dB drop off points. It can be modeled by a 20-pole Chebyshev bandpass filter which has a transfer function as shown

$$|H_n(j\Omega)|^2 = \frac{1}{1+\epsilon^2 T_n^2(\Omega)} \tag{28}$$

where $T_n(\omega)$ is the nth Chevbyshev polynomial, and ε determines the amplitude of the ripple in the passband of the filter. Reference [10] has shown that this filter can be approximated by a brick-wall bandpass filter. Therefore, Eqn. (27) can be rewritten as

$$PWC = \int_{f_c-BW}^{f_c+BW} S(f)\, df \tag{29}$$

where BW is the one-sided bandwidth of the SAW filter Observe that Eqn (29) is correct since S(f) given by Eqns (14) and (18) arc one-sided PSDs and the equivalent low pass filter of the bandpass filter is considered in Eqn (29), Evaluating Eqn (29) for a specified power containment (PWC) is nearly impossible since n is not known and nor is f_{sc}. in addition, one can interactively estimates n but for each estimate the integral in equation (29) must be evaluated from f_c-BW to f_c+BW which is a time consuming process for large bandwidth, BW. One wishes, therefore, to have a mathematical model in a closed form that can provide an accurate estimate of the upper bound value of n_M that requires the less computational time (and which works for predetection filter bandwidth, BW). in

the following, a simple method is developed to approximate the upper bound value n_M, and the accuracy of this model will be verified latter in the numerical results section by actual calculation of Eqn. (29).

The upper bound for n_M for both square wave and sine wave subcarrier cases can be computed from

$$BW = h(n_M R_S) + kR_S \tag{30}$$

with the assumption that

$$f_{SC} = n_M R_S \tag{31}$$

and n_M is an integer. Solving for n_M one obtains

$$n_M = \left(\frac{BW}{R_S} - k\right)_h \tag{32}$$

where h is the harmonic order of the data spectrum to be enclosed within the filter bandwidth and k is the number of right-sided sidelobes of the hth order harmonic to be enclosed in the filter bandwidth. One can choose k as an integer or a decimal number, but the latter would results in a small deviation from the true estimate in exchange for shorter computation time. in order to compute n_M, one must first determine the parameters k and h. This is possible once the percentage of power contains within the filter bandwidth is specified. To simplify the calculation of parameter h, one would, first, need to assume infinite number of sidelobes for each of the data harmonics in the calculation. This assumption will be rectified partially at the evaluation of the parameter k. With

this assumption, the parameter h is determined for the sinewave subcarrier from

$$PWC_0(h) = \left(\frac{1}{\sum_{i=1,3,5,\ldots}^{\infty} J_i^2(m)} \sum_{i=1,3,5,\ldots}^{h} J_i(m) \int_{-\infty}^{\infty} S_D(f - i f_{fsc})\, df \right) \tag{33}$$

and for square wave subcarrier it is determined by

$$PWC_1(h) = \left(\frac{8}{\pi^2} \sum_{i=1,3,5,\ldots}^{h} \frac{1}{(i)^2} \int_{-\infty}^{\infty} S_D(f - i f_{sc})\, df \right) \tag{34}$$

Evaluating integrals in Eqns. (33) and (34), one obtains the simplified forms as shown respectively below

$$PWC_0(h) = \frac{\sum_{i=1,3,5,\ldots}^{h} J_i^2(m)}{\sum_{i=1,3,5,\ldots}^{\infty} J_i^2(m)} \tag{35}$$

$$PWC_1(h) = \frac{8}{\pi^2} \sum_{i=1,3,5,\ldots}^{h} \frac{1}{i^2} \tag{36}$$

From Eqns. (35) and (36), one can determine the minimum parameter h that is required to obtain approximately the given PWC. To correct the assumption that the prc-filtering bandwidth is unlimited one observes that, as shown in Fig. (2), only k numbers of sidelobes of the data's hth harmonics arc needed to meet the required PWC. One can determine this parameter simply by iteractively evaluated Eqn (37) until a value for k can be found to satisfy the specified PWC.

$$PWC_{correct} = \int_{-BW}^{kR_s} SD(f)\, df \approx \frac{1}{2} + \int_{0}^{kR_s} S_D(f)\, df \qquad (37)$$

where $S_D(f)$ is the data PSD at baseband defined in Eqn. (6). Once the parameters h and k are obtained, the upper bound n_M, can be calculated easily from Eqn. (32). The estimated total power containment within the specified pre-filter bandwidth (BW), PWC_{EST}, corresponding to n_M is given by

$$PWC_{EST} \approx \begin{cases} PWC_j(\cdot) \cdot PWC_{correct} & ; h = 1 \\ PWC_j(h-2) + PWC_j(j=h) \cdot PWC_{correct} & ; h > 1 \end{cases} \qquad (38)$$

for j= O corresponds to sine wave, anti 1 for square wave subcarrier. The actual value of the total power containment for a given n_M can be obtained by substituting n_M into Eqn. (31) and evaluating Eqns (31) and (27) for PWC. Numerical results will be shown in the following sections to confirm the accuracy of the model. The specifications used in the calculation pertains to the DSN/Block IV and V receiver systems.

V. SIMULATION

A direct approach to obtain the lower bound n_L is by computer simulation. This approach will be used to verify the presented mathematical models. The communication systems under investigation are simulated using Comdisco's Signal Processing Workstation (SPW) software. Figures 3 and 4 show the block diagram for the systems of square wave and sine wave subcarriers respectively. Basic operation of these systems are described below.

The PLL receives the PCM/PSK/PM/NRZ/Square-wave or PCM/PSK/PM/NRZ/Sine-wave signal from the Test Signal Generator (TSG). Due to data interfering with the carrier, the PLL will output an imperfect reference of the carrier as defined in Eqn. (9). The imperfect carrier is then

used to demodulated the data signal which, using Eqns. (2) and (3), can be modeled for the square wave and sine wave subcarriers respectively as

$$I(t)_{SQUARE} = \sqrt{2P_T}d(t)\sin(m)\cos(\omega_c t) + n(t) \quad (39)$$

$$I(t)_{SINE} = \sqrt{2P_T}d(t)\left(\sqrt{2}J_1(m)\sin(\omega_c t)\right) + n(t) \quad (40)$$

where n(t) is a while gaussian noise. The demodulated signals are then filtered to produce the corrc.spending baseband signals

$$I(t)_{SQUARE} = \sqrt{P_T}\sin(m)\,d(t)\cos(\phi(n,t)) + n_{LPF}(t) \quad (41)$$

$$I(t)_{SINE} = \sqrt{P_T}\left(\sqrt{2}J_1(m)\right)d(t.)\cos(\phi(n,t)) + n_{LPF}(L) \quad (42)$$

These basband signals are then filtered by a match filter to reproduce the transmitted data symbol. Since there is noise in the signal and the carrier tracking is imperfect, the reproduced data symbol may not match with the transmitted data symbol. in this case, an error has occurred; hence, an error counter is employed to count the number of times this happens, Knowing this number the SER can be computed using the equation

$$P_{esim} = \frac{NR_S}{J_t f_s} \quad (43)$$

where N denotes the number of symbol error detected, R_s is the symbol rate, 1, is the total number of iteration points run for the simulation, and f_s is the sampling frequency. The subsequent section presents simulation results obtained from the simulation systems shown in Figs. (3)-(4). Note that by simulating the systems shown in Figs. (3)-(4) one. has assumed that the subcarrier tracking is perfect which is consistent with the mathematical models presented in Section 3.

VI. NUMERICA 1. RESULTS

Two types of data will be presented here to determine the bounds for n, onc comes from the theories described above and the other comes from computer simulation. These data will be presented jointly for comparison purposes,

For the square wave subcarrier, the simulated case is for B_L/R_S '- 0.5, tracking loop bandwidth is 150 Hz [9], and the corresponding bit rate is 300 bit-per-second. Using Eqns. (22) and (23) the bit error rate is computed. Figures (5a) and (5b) shows the SER versus the symbol SNR from the simulation and simulation plus calculation respectively. As illustrated by the arrows, the differences in the symbol SNR between the curves of "Ideal" and the curve of "n = ∞" represent the radio loss as defined in [1]. Note that the curve labeled "Ideal" denotes for the case when the loop SNR and n are infinite. The symbol SNR degradation due to data interference can be found by measuring the horizontal distance between the curve of "n=∞" to the corresponding curve of n for a fixed value of SER. in Fig. (5b), the simulation and the theory datum are plotted jointly to show that the as n gets larger, the results from theory and simulation ai c more agreeable.

Figures (6a) and Fig. (6b) depict SER curves for B_L/R_S = 2.5, plotted for the simulation and theory plus simulation data respectively, At this B_L/R_S ratio, the data interference can not be considered as white noise for low value of n. In these cases, results from the simulation will be used to determine the minimum value of n. Figures (7a) and (7b) depict SER curves for B_L/R_S = 4.69. Note. that for the latter two cases, the theoretical results for the SER arc obtained from calculating, Eqns. (25) and (26).

Using the loop bandwidth-to-sy mbol rate ratio (B_L/R_s) values of the square wave subcarrier case, the SER for the sine wave subcarrier case were calculated and ploted against symbol SNR as shown in Figures 8, 9, and 10. Note that for the two cases of B_L/R_s = 2.5 and 4.69, higher order of

the carrier harmonics do fall into the carrier tracking loop bandwidth for low values of n (i.e. n = 1, 2, or 3.) For these cases, the SER were obtained from calculating equation (25) and (26) and the results were verified by computer simulation.

From these Figures, one can see that in order to minimize symbol SNR degradation due to data interference, one would need a certain minimum value of n. This is the lower bound n_L. Table I summarizes the minimum value of the subcarrier frequency-to-bit rate ratio, n_L, that result in the Symbol SNR degradation of 0.1 dB or less.

TABLE 1. MINIMUM VALUE OF THE SUBCARRIER FREQUENCY-TO-SYMBOL RATE RATIO, N_L, FOR SER $\leq$ 10-3 WITH THE SYMBOL SNR DEGRADATION OF 0.2 dB OR LESS

MODULATION TYPE	PCM/PSK/PM/SQUARE-WAVE			PCM/PSK/PM/SINE-WAVE		
B_L/R_S	4.69	2.5	$\leq$ 0.5	4.69	2.5	$\leq$ 0.5
$n_L = f_{SCL}/R_S$	10	10	3	10	10	3
SSNR Degradation in dB	$\leq$ 0.19 dB	$\leq$ 0.1 dB	$\leq$ 0.1 dB	$\leq$ 0.16 dB	$<$ 0.1 dB	$<$ 0.1 dB

The upper bound of n, n_M, can be calculated by Eqn. (30). Here, the prc-filter is taking as the pi-c-filtering filter of the block V receiver [8], the bandpass SAW filter. This filter has a pass band of 66MHz; measured between the -1 dB drop off points. Using Eqns. (32) and (38), the maximum value for the parameter of n was calculated for two values of the data power containment and the results are verified by using Eqn. (29). The results are tabulated in Tables (2)-(5) for both sine-wave and square-wave subcarrier. Note that the column contained the "Estimated Value" is calculated from Eqns (32) and (38). While the column labeled "Actual Value" is computed from Eqn. (29). Depending on the amount of the desired power containment, the upper bound for the subcarrier frequency-to-bit rate ratio can be selected from these tables.

TABLE 2. MAXIMUM (UPPER BOUND) VALUE OF THE SUBCARRIER FREQUENCY-TO-SYMBOL RATE RATIO, n_M FOR TWO VALUES OF POWER CONTAINMENT AT 500 K SYMBOLS PER SECOND (SPS)

R_S = 500 Ksps								
	PCM/PSK/PM/SQUARE WAVE				PCM/PSK/PM/SINE WAVE			
n_M	9		4		65		56	
PWC %	Estimated Value	Actual Value	Estimated Value	Actual Value	Estimated Value	Actual Value	Estimated Value	Actual Value
	94.93	95.16	97.5	97.71	94.02	93.98	98.32	98.66

TABLE 3. MAXIMUM (UPPER BOUND) VALUE OF THE SUBCARRIER FREQUENCY-TO-SYMBOL RATE RATIO, n_M FOR TWO VALUES OF POWER CONTAINMENT AT 300 SYMBOLS PER SECOND (SPS)

R_S = 300 SPS								
	PCM/PSK/PM/SQUARE WAVE				PCM/PSK/PM/SINE WAVE			
n_M	15714		4074		109999		109991	
PWC %	ESTIMATED VALUE	ACTUAL VALUE	ESTIMATED VALUE	ACTUAL VALUE	ESTIMATED VALUE	ACTUAL VALUE	ESTIMATED VALUE	ACTUAL VALUE
	94.92	95.29	98.55	98.94	94.73	94.68	99.01	98.96

TABLE 4. MAXIMUM (UPPER BOUND) VALUE OF THE SUBCARRIER FREQUENCY-TO-SYMBOL RATE RATIO, n_M FOR TWO VALUES OF POWER CONTAINMENT AT 60 SYMBOLS PER SECOND (SPS)

R_S = 60 sps								
	PCM/PSK/PM/SQUARE WAVE				PCM/PSK/PM/SINE WAVE			
n_M	78571		23912		549999		549995	
PWC %	ESTIMATED VALUE	ACTUAL VALUE	ESTIMATED VALUE	ACTUAL VALUE	ESTIMATED VALUE	ACTUAL VALUE	ESTIMATED VALUE	ACTUAL VALUE
	94.93	95.31	98.31	98.700	95.12	95.07	98.97	98.92

TABLE 5. MAXIMUM (UPPER BOUND) VALUE OF THE SUBCARRIER FREQUENCY-TO-SYMBOL RATE RATIO, n_M FOR TWO VALUES OF POWER CONTAINMENT AT 32 SYMBOLS PER SECOND (SPS)

R_S = 32 sps								
	PCM/PSK/PM/SQUARE WAVE				PCM/PSK/PM/SINE WAVE			
n_M	147321		33266		1031249		1031245	
PWC %	Estimated Value	Actual Value	Estimated Value	Actual Value	Estimated Value	Actual Value	Estimated Value	Actual Value
	94.93	95.31	98.73	99,13	95.14	95.09	98.99	98.94

VII. SUMMARY ANI) CONCI,1IS1ONS

This paper has analyzed the performance of the PCM/PSK/PM receiver for both square and sine wave subcarrier. The performance of the receivers under investigation is characterized by (a) the SER performance, and (b) the amount of the data recovered from the first IF stage filtering (or the total data power contained in the filtered bandwidth). Both SER ant] total data power containment are computed as a function of the subcarrier frequency-to-symbol rate ratio, n. Based on the SER performance, one

can establish the lower bound (or minimum) value n_L. On the other hand, the upper bound (or maximum) n_M, is determined from the required data power containment in the first IF stage filter bandwidth. The specifications on the loop bandwidth, minimum and maximum data rate, and the bandwidth of the first stage IF filter are obtained from the DSN/Block IV and V receivers. These specifications are used in the theoretical calculations of the SER and data power containment (or recoverable data power) in the filter bandwidth. The theoretical results are then verified by computer simulation .

Both theoretical and simulation results show that, for $B_L/R_S \leq 0.5$ and SER $\leq 0^{-3}$, the lower bound for n is 3 (i. e., $n_L = 3$) for both square and sine wave subcarriers. For $0.5 < B_L/R_S \leq 4.7$, the lower bound for n is found to be 10. When the subcarrier frequency is chosen to be exactly at $n_L R_S$, a symbol SNR degradation of 0.2 dB or less occurs. 'l'able 6 summarizes the results for lower bound values of n_L.

The maximum (or upper bound) value n_M is determined from a 95'% of total data power containment in the first stage IF filter bandwidth. Using the results presented in Tables 2-5, the log of n_M as function of the symbol rate is plotted in Fig. 11 for both square wave and sine wave subcarriers. For a fixed IF filter bandwidth, figure 11 shows that as one increases the data rate one has smaller upper bound n_M.

TABLE 6. RECOMMENDED MINIMUM VALUES FOR THE SUBCARRIER FREQUENCY TO-SYMBOL-RATE RATIO FOR SER $\leq$ 10-3 WITH SYMBOL SNR DEGRADATION OF 0.2 dB OR LESS.

Operating Conditions	$B_L/R_S \leq 0.5$	$0.5 < B_L/R_S \leq 4.7$
Recommended Minimum n_1, n_2	3	10

ACKNOWLEDGMENT

The work described in this paper was carried out by the Jet Propulsion Laboratory, California institute of Technology, under contract with the National Aeronautics and Space Administration.

REFERENCES

[1] J. Yuen, Deep Space Telecommunications Systems Engineering, Plenum Press, 1983,

[2] M. M. Shihabi, "P. M. Nguyen and S. M. Hinedi, "A Comparison of Telemetry Signals in the Presence and Absence of a Subcarrier," IEEE Transactions on EMC, Vol. 36, No. 1, pp. 1-13, February 1994,

[3] consultative Committee for Space Data Systems, Recommendations for Space Data System Standards, Radio Frequency and Modulation Systems, Part 1, Earth Stations and Spacecraft, CCSDS 401.0-B, Blue Book, Washington, DC: NASA, CCSDS Secretariat, Communications and Data Systems Division (Code OS), 1989.

[4] J. K.. Holmes, Coherent Spread Spectrum Systems, New York: John Wiley and Sons, 1982.

[5] Tien M. Nguyen, "Closed Form Expressions for Computing the Occupied Bandwidth of PCM/PSK/PM Signals," Proceedings of the IEEE International Symposium on EMC, Cherry Hills, New Jersey, August 1991.

PCM/PSK/PM Signals," Proceedings of the IEEE international Symposium on EMC, Cherry Hills, New Jersey, August 1991.

[6] Tien M. Nguyen, "Occupied Bandwidths for PCM/PSK/PM and PCM/PM Signals---A comparative Study," International Consultative Committee for Space Data Systems, Subpanel 1E, RF and Modulation Meeting, Salzburg, Austria, May 1992.

[7] W. C. Lindsey and M.K. Simon, Telecommunications Systems Engineering, Englewood Cliffs, New Jersey: Prentice-Hall, 1973,

[8] "Digital filter to simulate the SAW bandpass filter in the Block V receiver", M. Aung, J. K, Holmes, IOM 3338-91-021

[9] Deep Space Network/Flight Project, Interface Design Handbook, Volume I: Existing DSN Capabilities, Document 810-5, Revision D, Volume 1, Jet Propulsion laboratory, Pasadena, California.

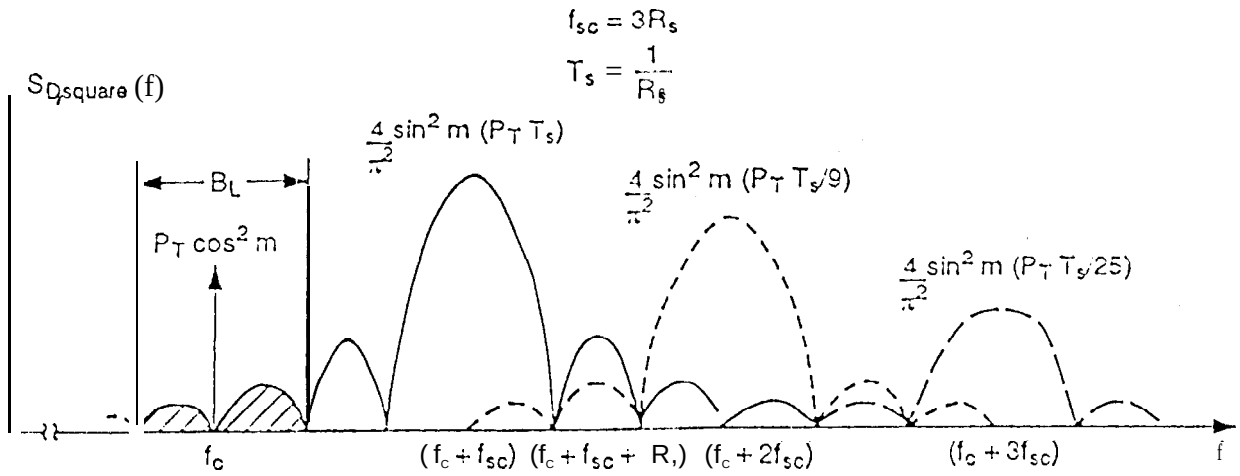

NOTE THAT THE POWER SPECTRUM ON THE LEFT OF THE RESIDUAL RF CARRIER f_c IS NOT SHOWN FOR THE SAKE OF CLARITY

(a)

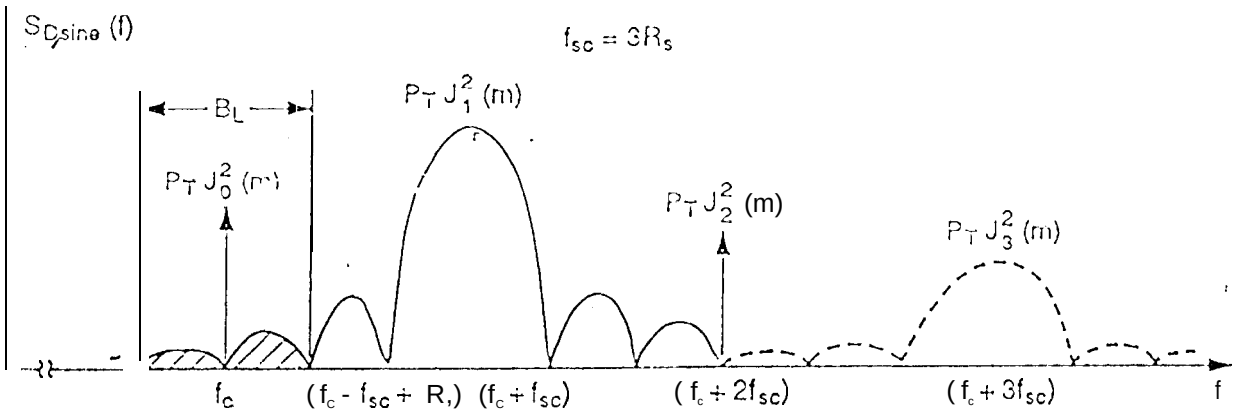

INOTE THAT THE POWER SPECTRUM CN THE LEFT OF THE RESIDUAL RF CARRIER f_c IS NOT' SHOWN FOR THE SAKE OF CLARITY

(b)

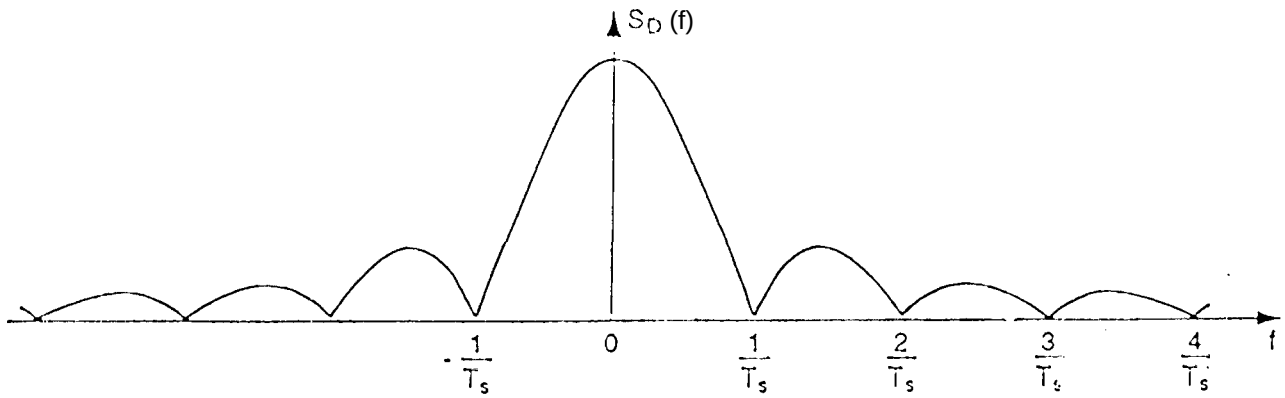

(c)

Figure 1. Power Density Spectrum of PCM/PSK/PM/NRZ: (a) with square wave subcarrier; (b) with sinewave subcarrier; (c) Data spectrum at baseband

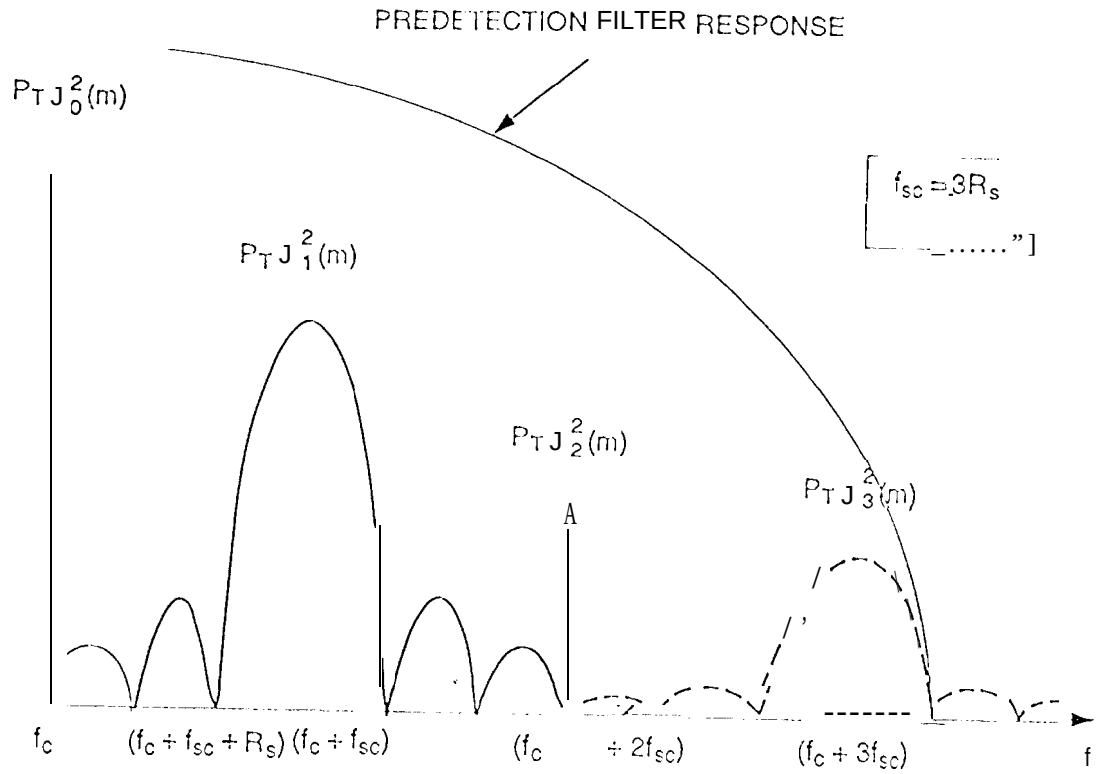

------- K = 1
-.-.-.- K = 2

NOTE THAT THE POWER SPECTRUM ON THE LEFT OF THE RESIDUAL RF CARRIER f_c IS NOT SHOWN FOR THE SAKE OF CLARITY

Fig. 2

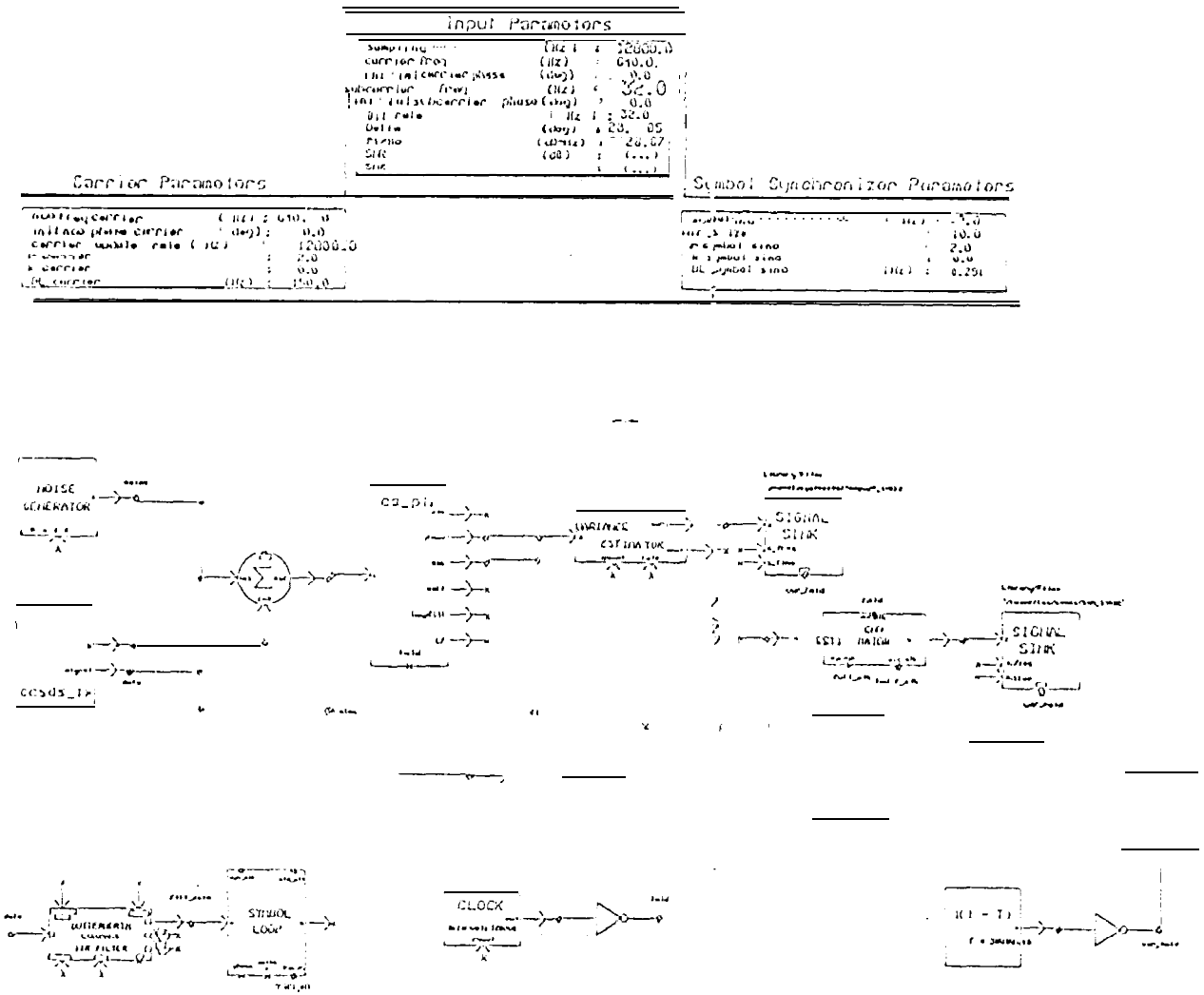

Figure 3. CCSDS DEMO OF PCM/PSK/PM/SQUARE-WAVE TRANSCEIVER

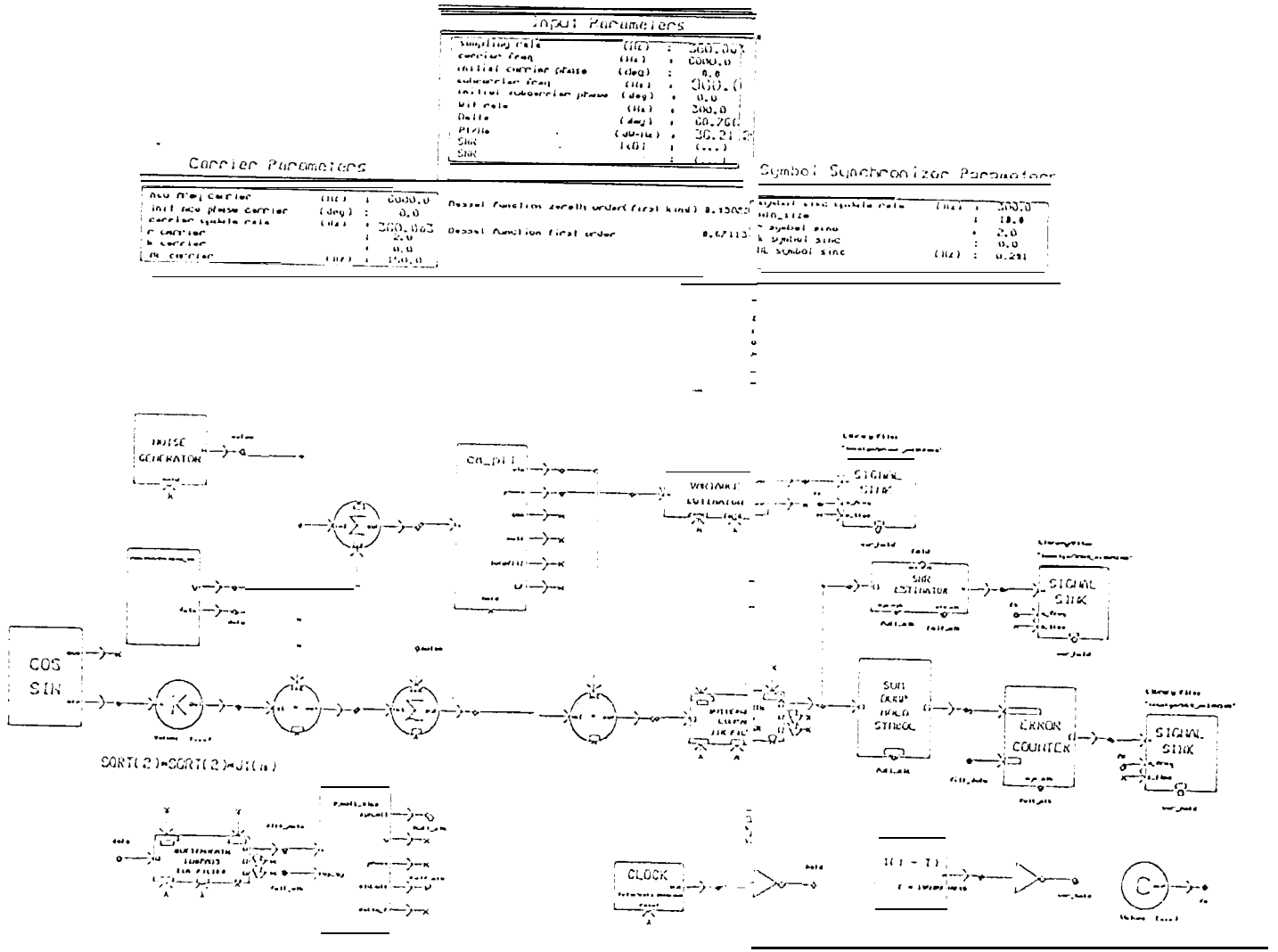

Figure 4. CCSDS DEMO OF PCM/PSK/PM/SINE-WAVE TRANSCEIVER

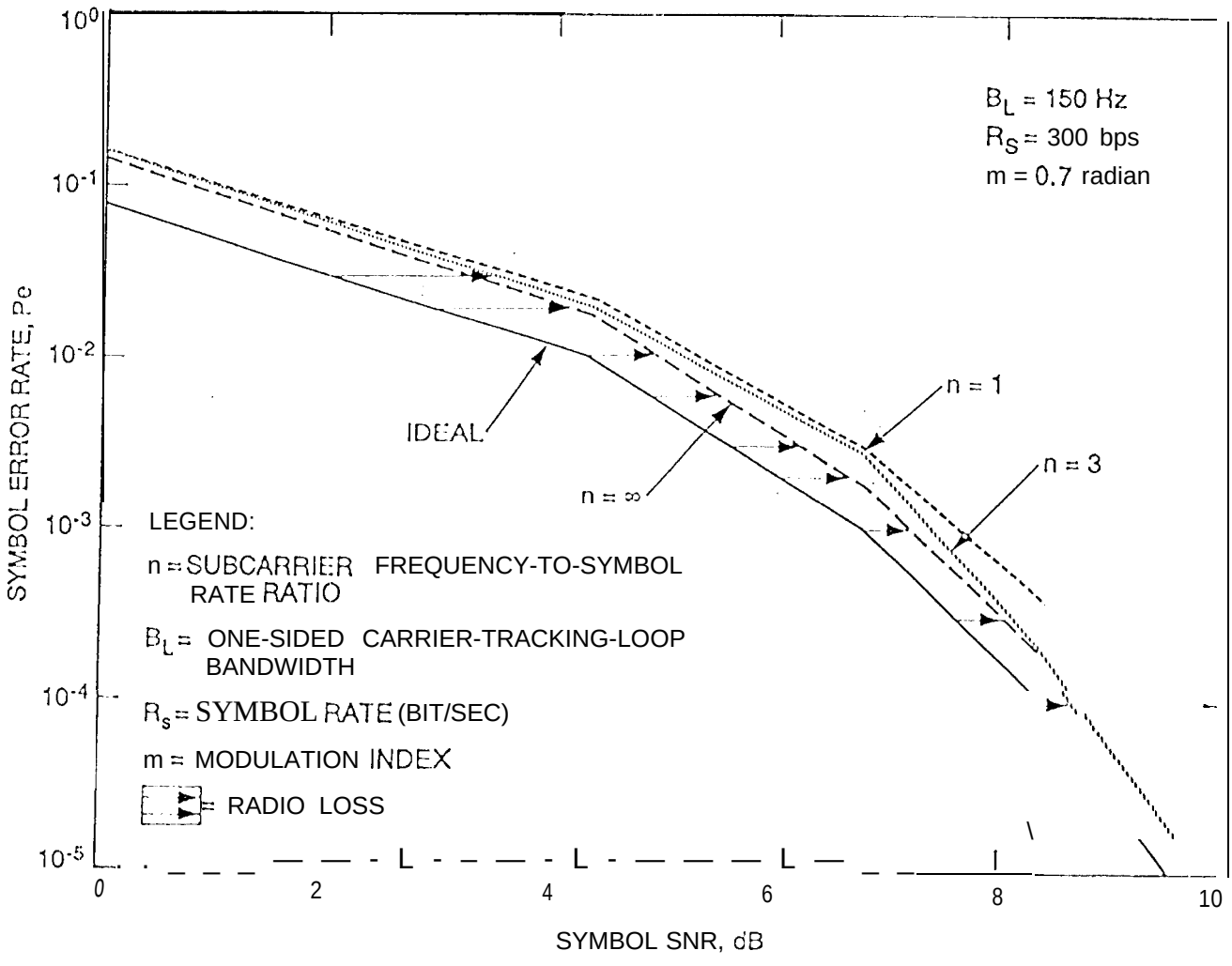

Figure 5a. Simulation SER vs Symbol SNR for PCM/PSK/PM/NRZ/Squarewave

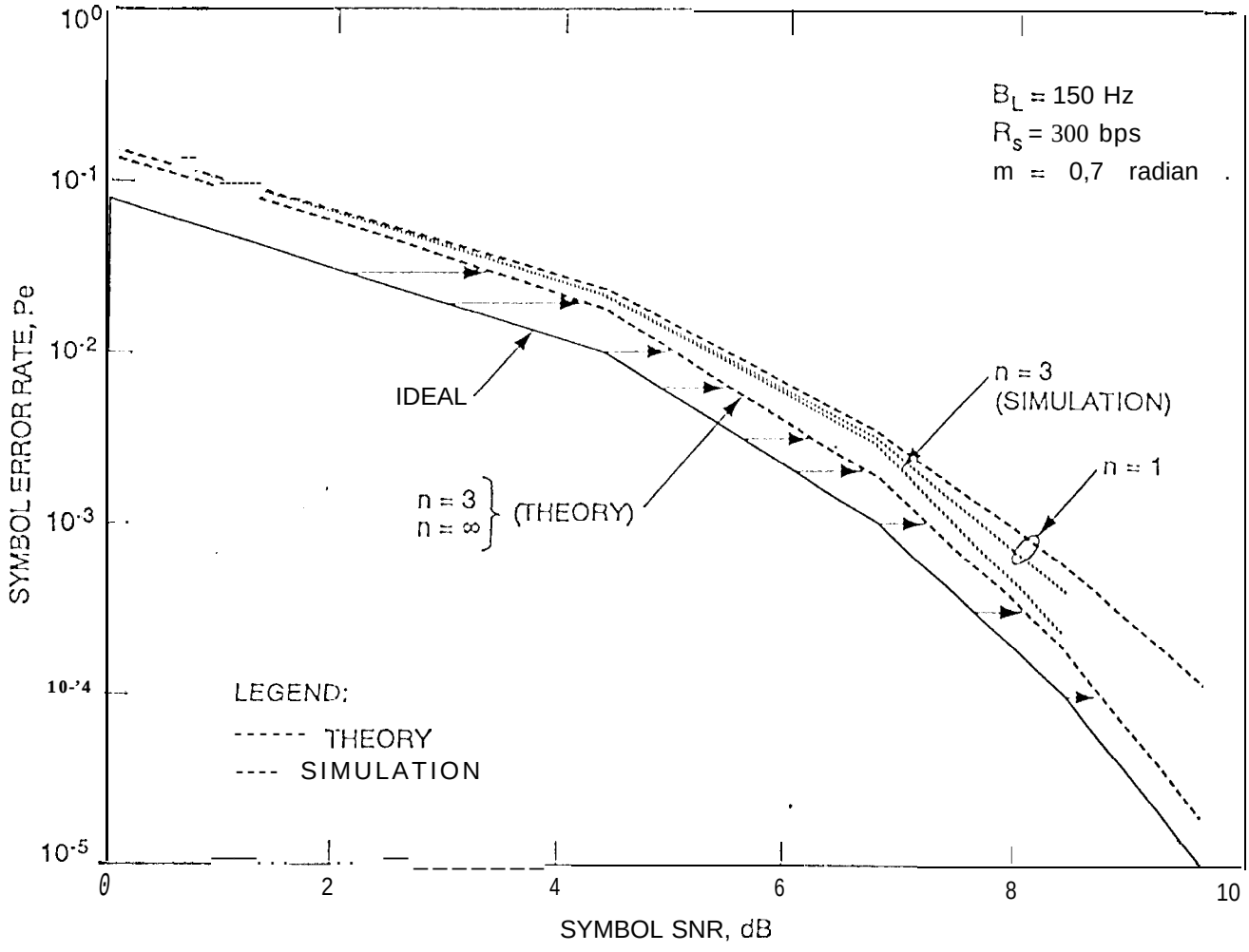

Figure 5b. Theory and Simulation SER vs Symbol SNR for PCM/PSK/PM/NRZ/ Squarewave

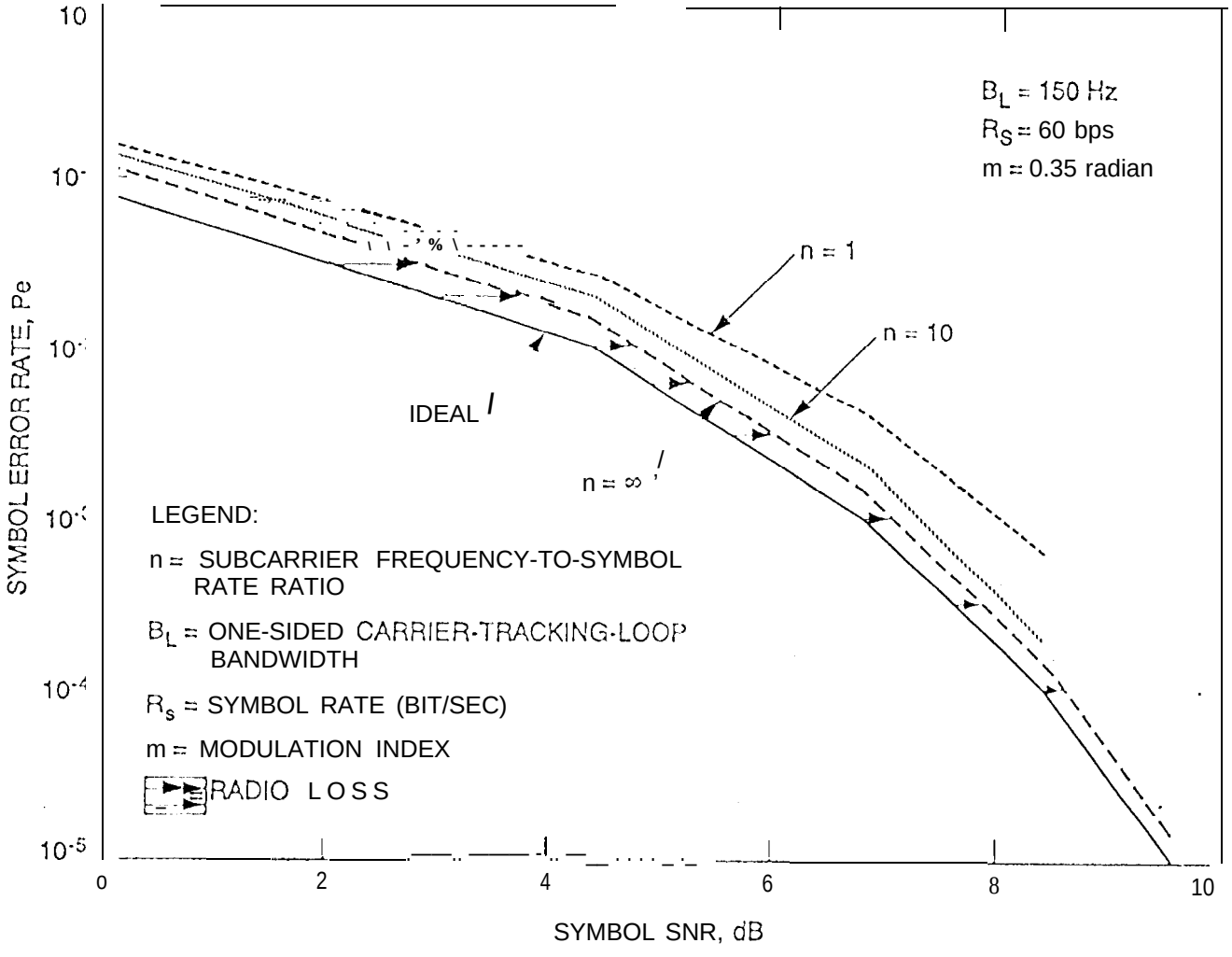

Figure 6a, Simulation SER vs Symbol SNR for PCM/PSK/PM/NRZ/Squarewave

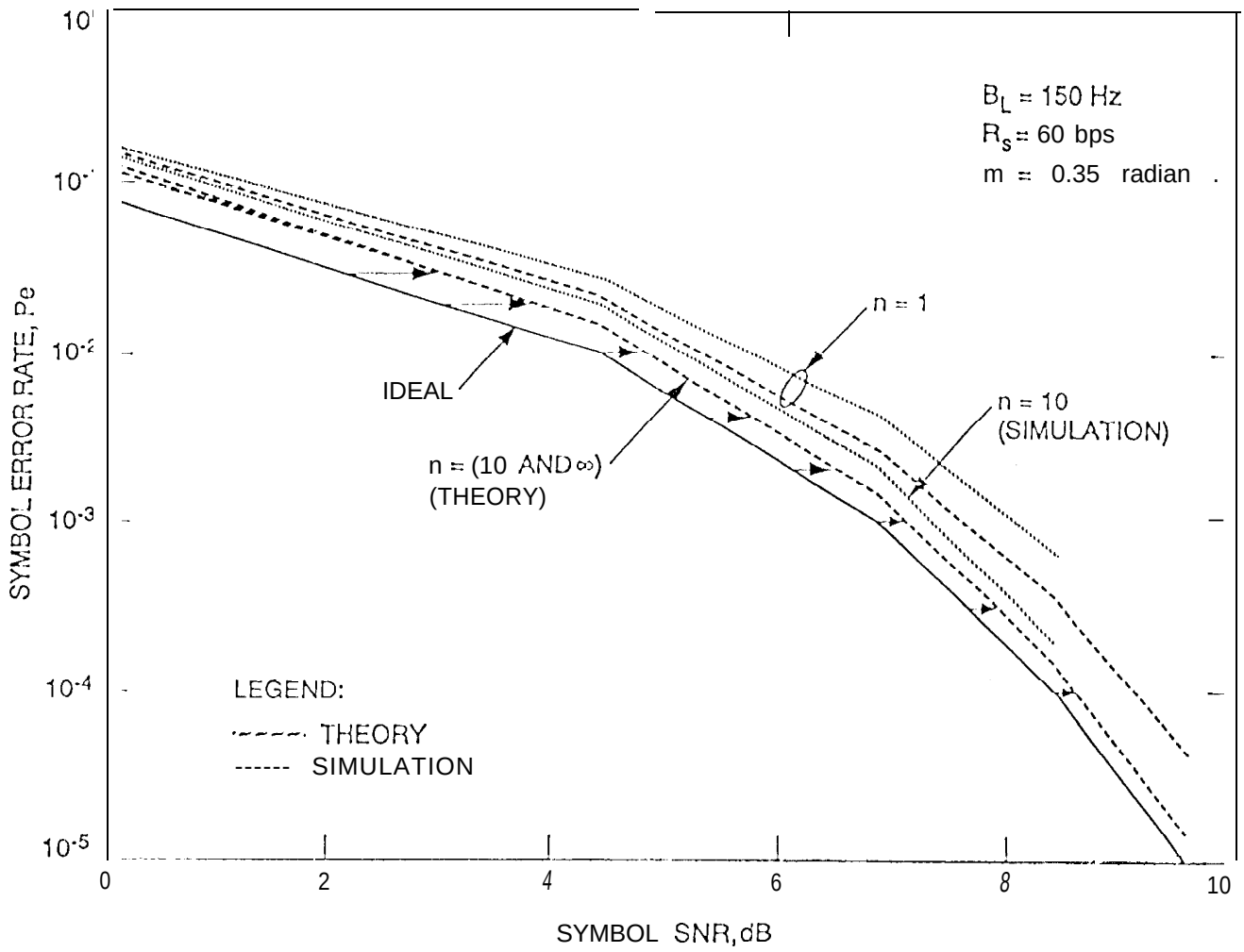

Figure 6b. Theory and Simulation SER vs Symbol SNR for PCM/PSK/PM/NRZ/Squarewave

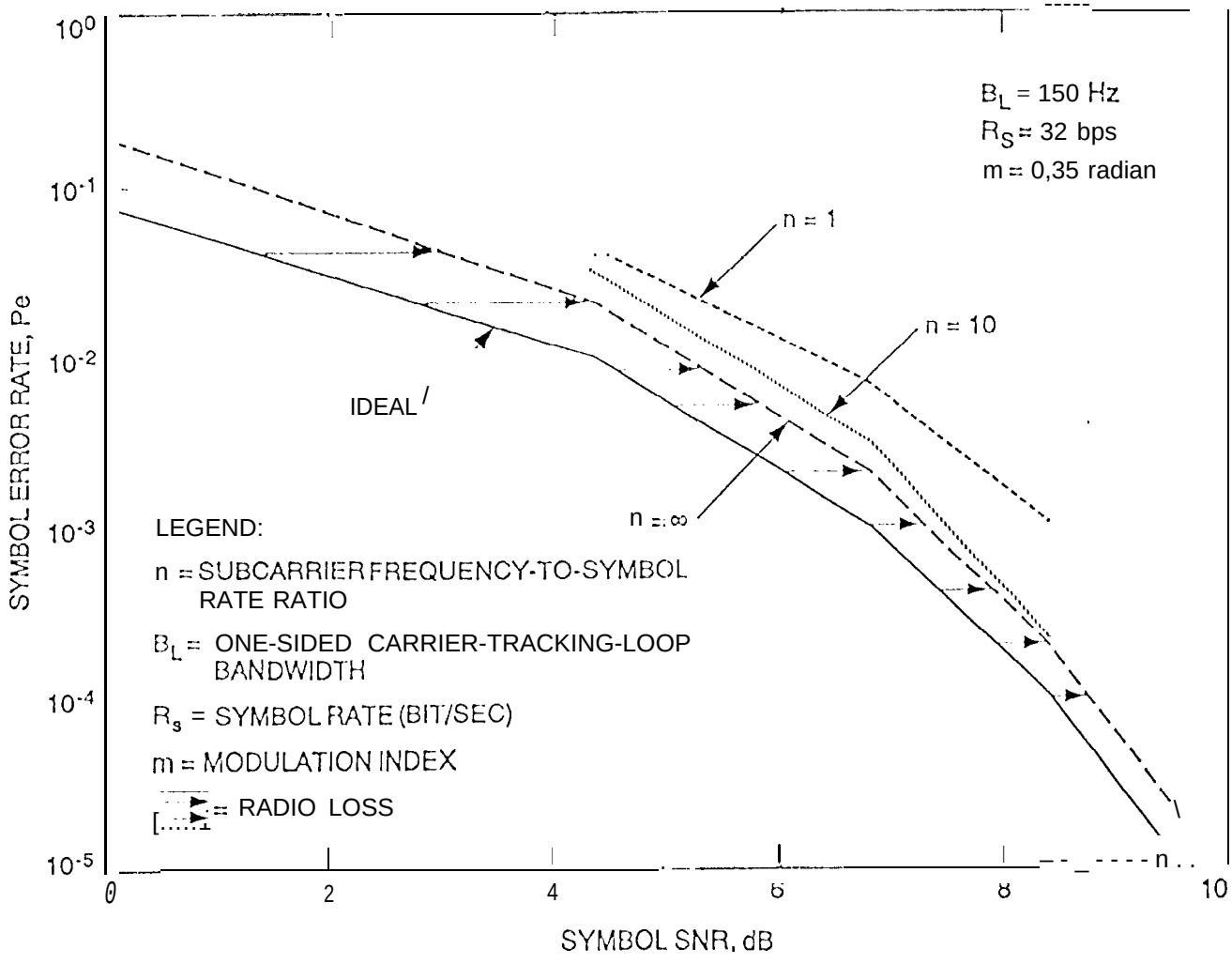

Figure 7a, Simulation SER vs Symbol SNR for PCM/PSK/PM/NRZ/Squarewave

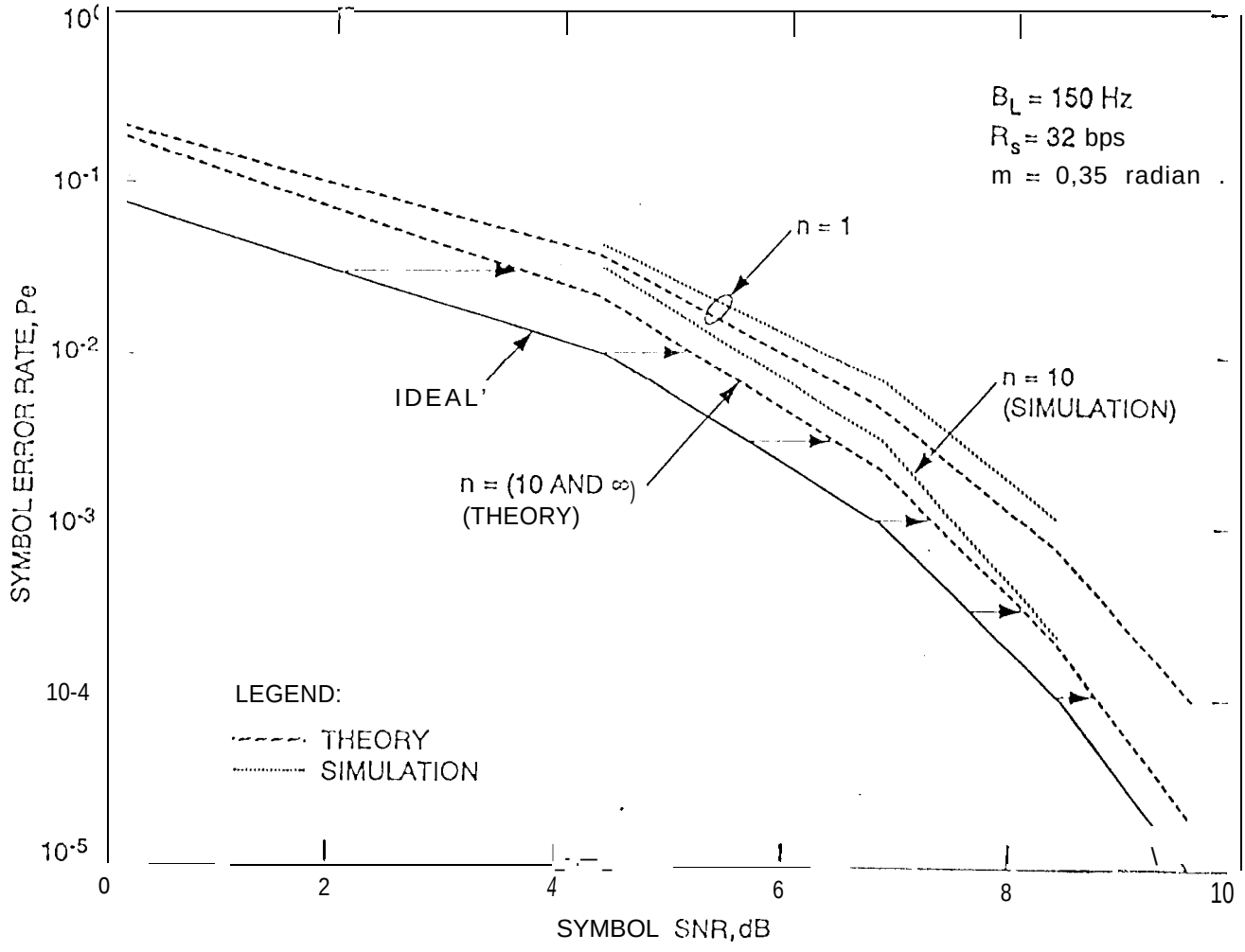

Figure 7b. Theory and Simulation SER vs Symbol SNR for PCM/PSK/PM/NRZ/ Squarewave

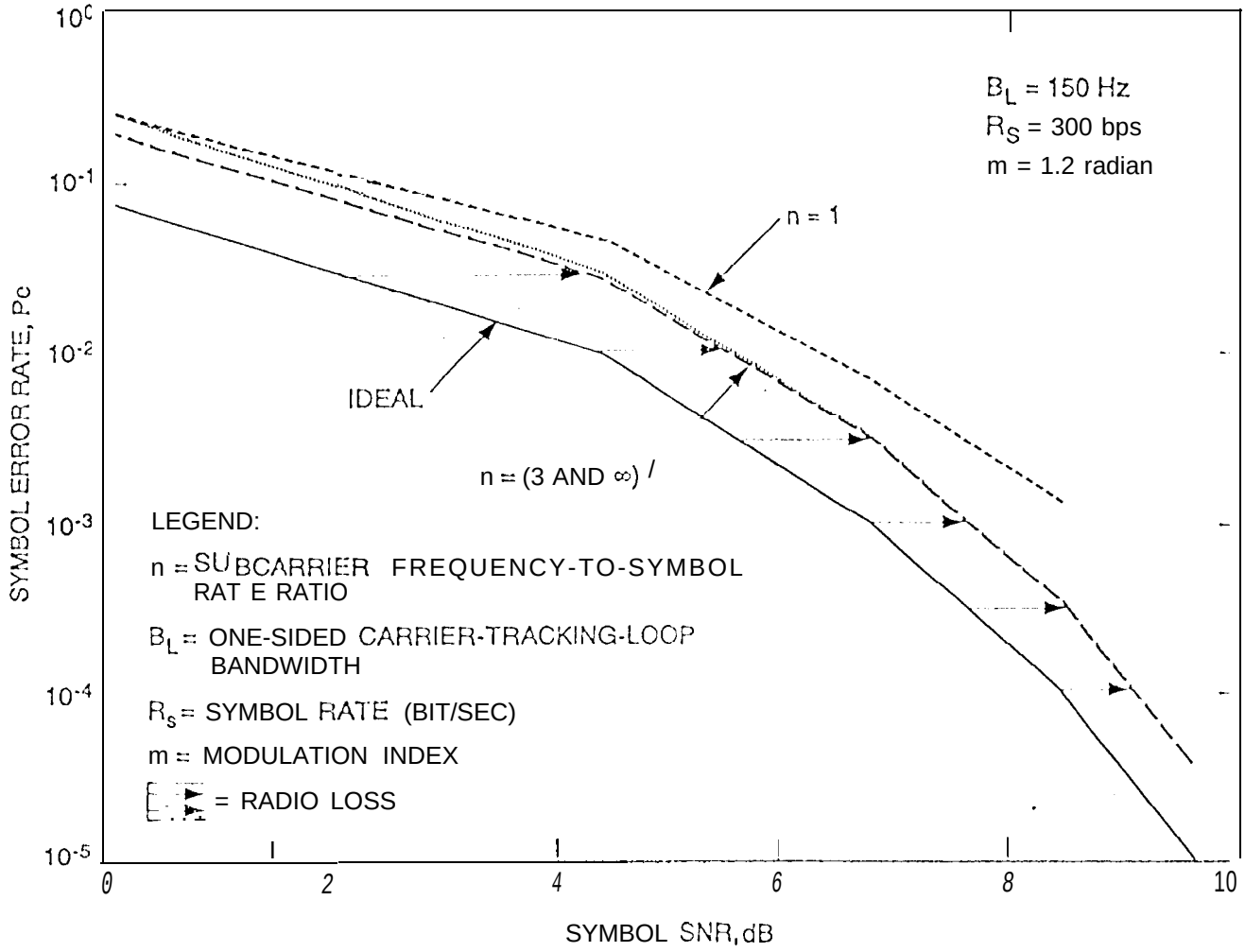

Figure 8a. Simulation SER vs Symbol SNR for PCM/PSK/PM/NRZ/Sinewave

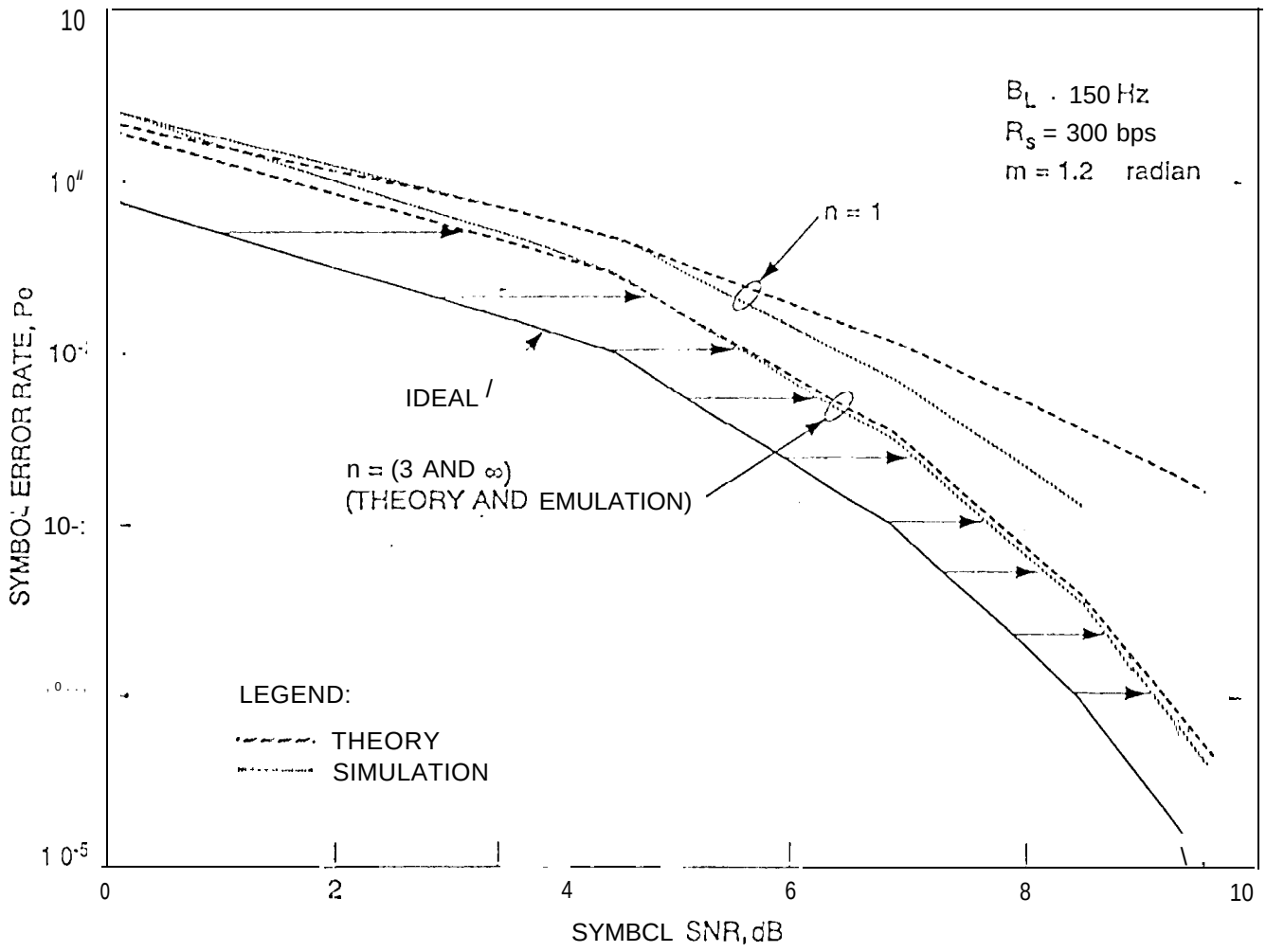

Figure 8b. Theory and Simulation SER vs Symbol SNR for PCM/PSK/PM/NRZ/ Sinewave

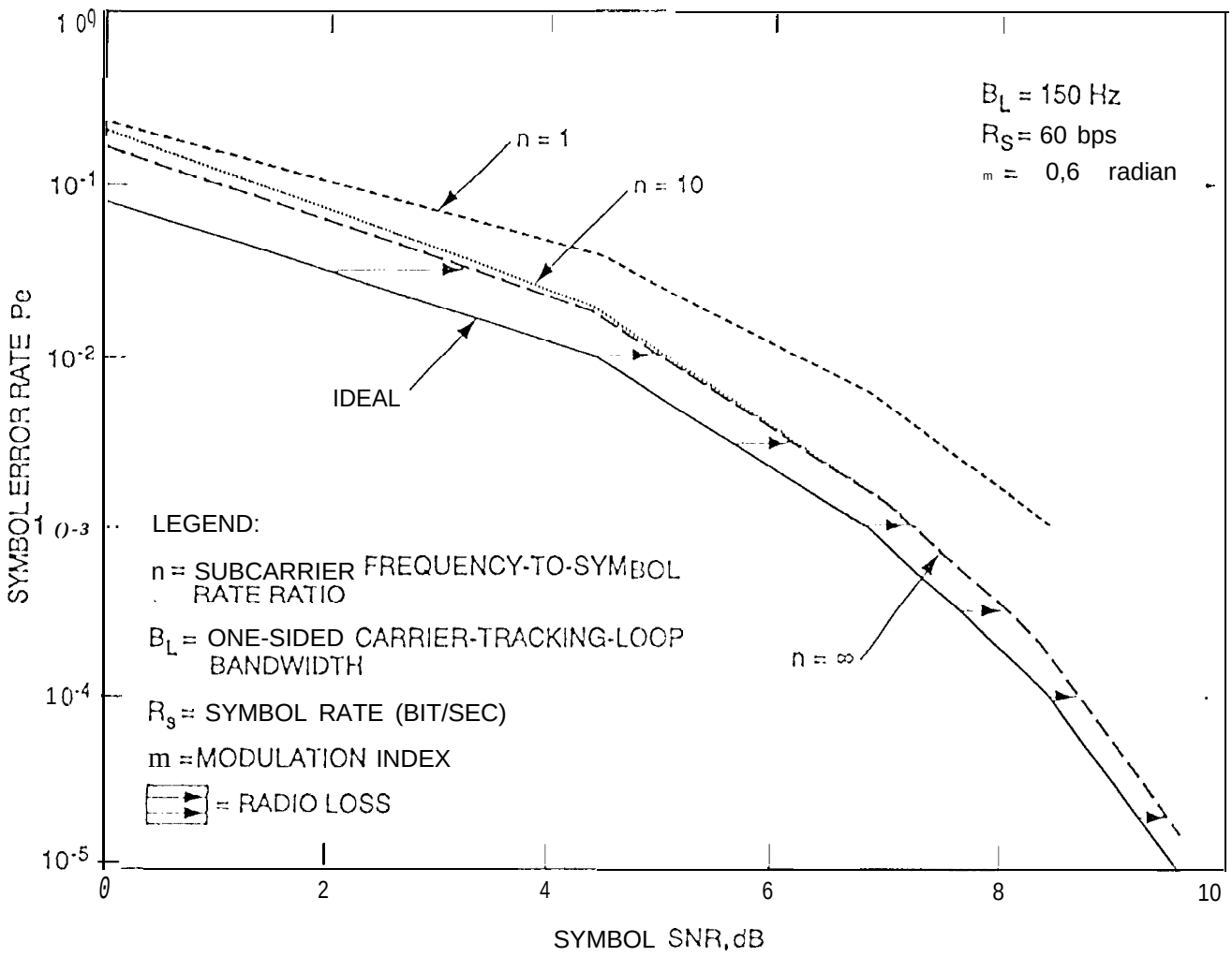

Figure 9a, Simulation SER vs Symbol SNR for PCM/PSK/PM/NRZ/Sinewave

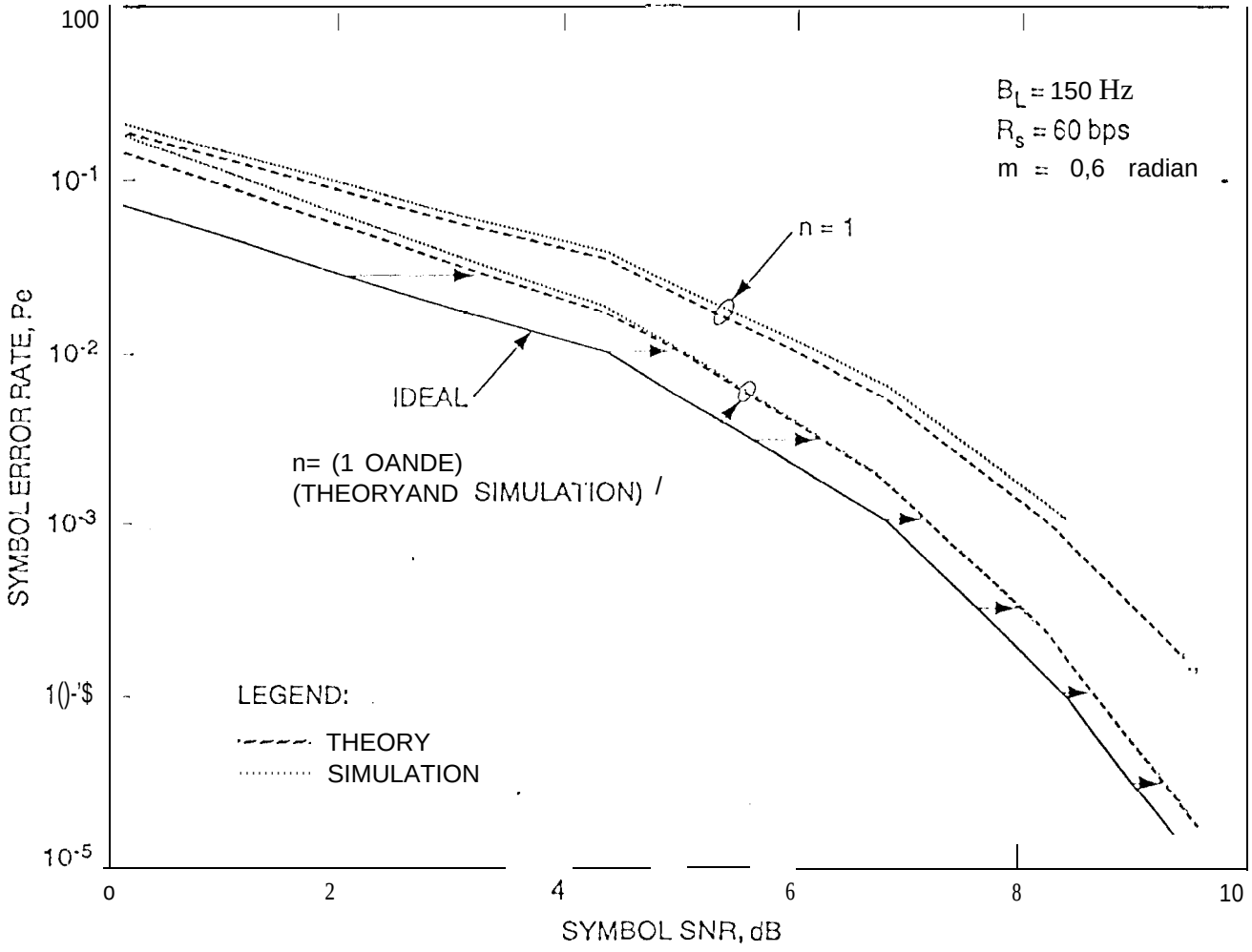

Figure 9b. Theory and Simulation SER vs Symbol SNR for PCM/PSK/PM/NRZ/ Sinews.ve

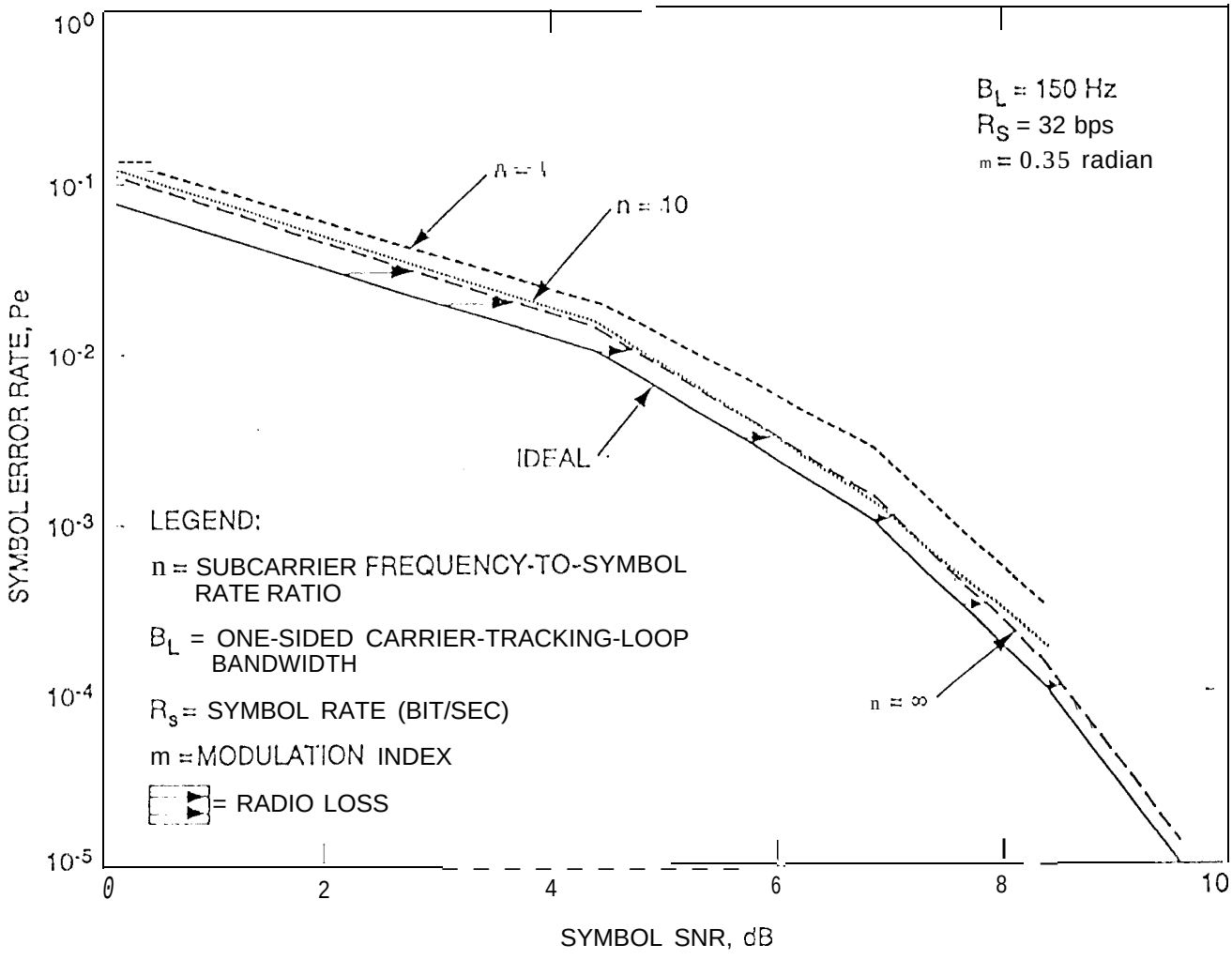

Figure 10a. Simulation SER vs Symbol SNR for PCM/PSK/PM/NRZ/Sinewave

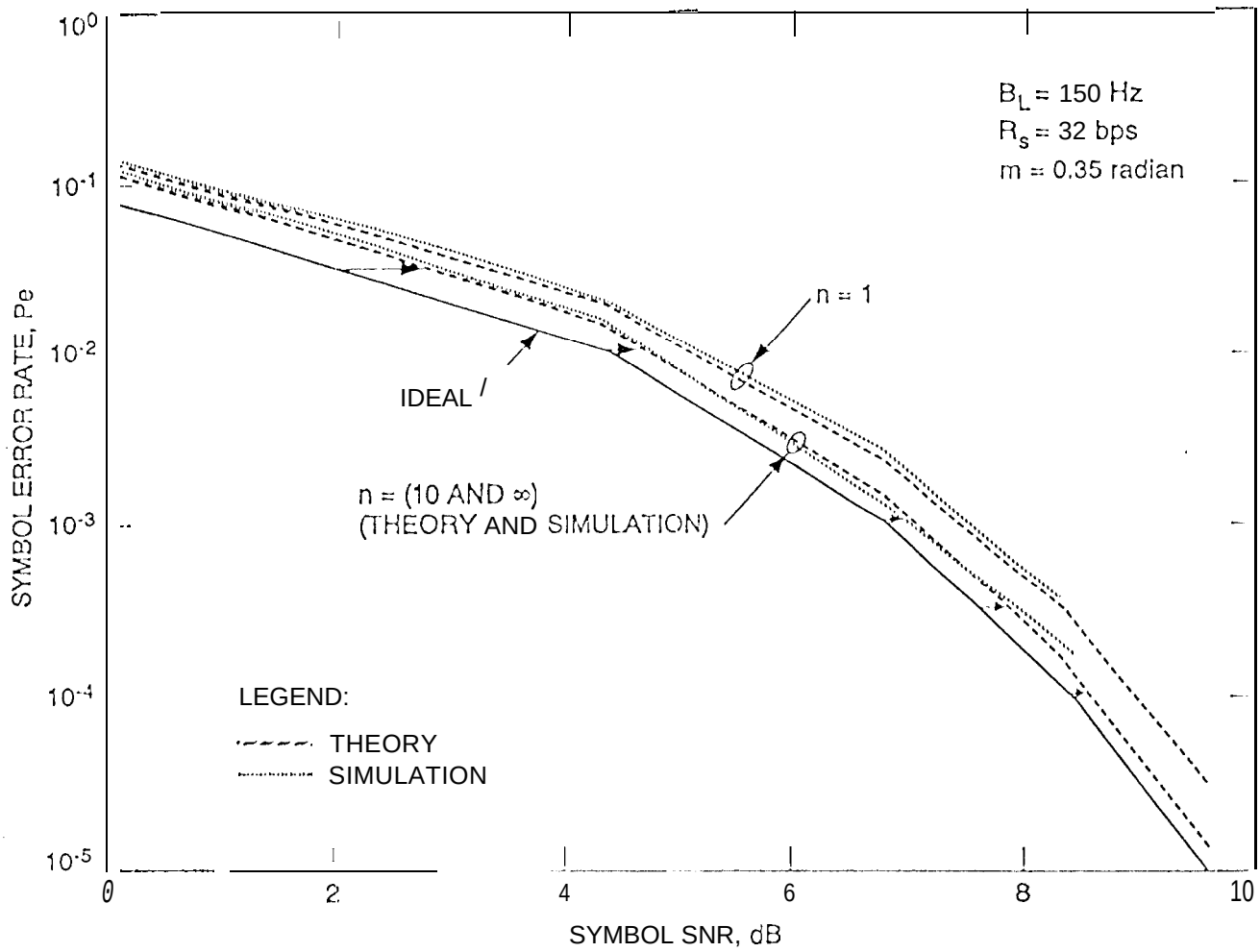

Figure 10b. Theory and Simulation SER vs Symbol SNR for PCM/PSK/PM/NRZ/ Sinewave

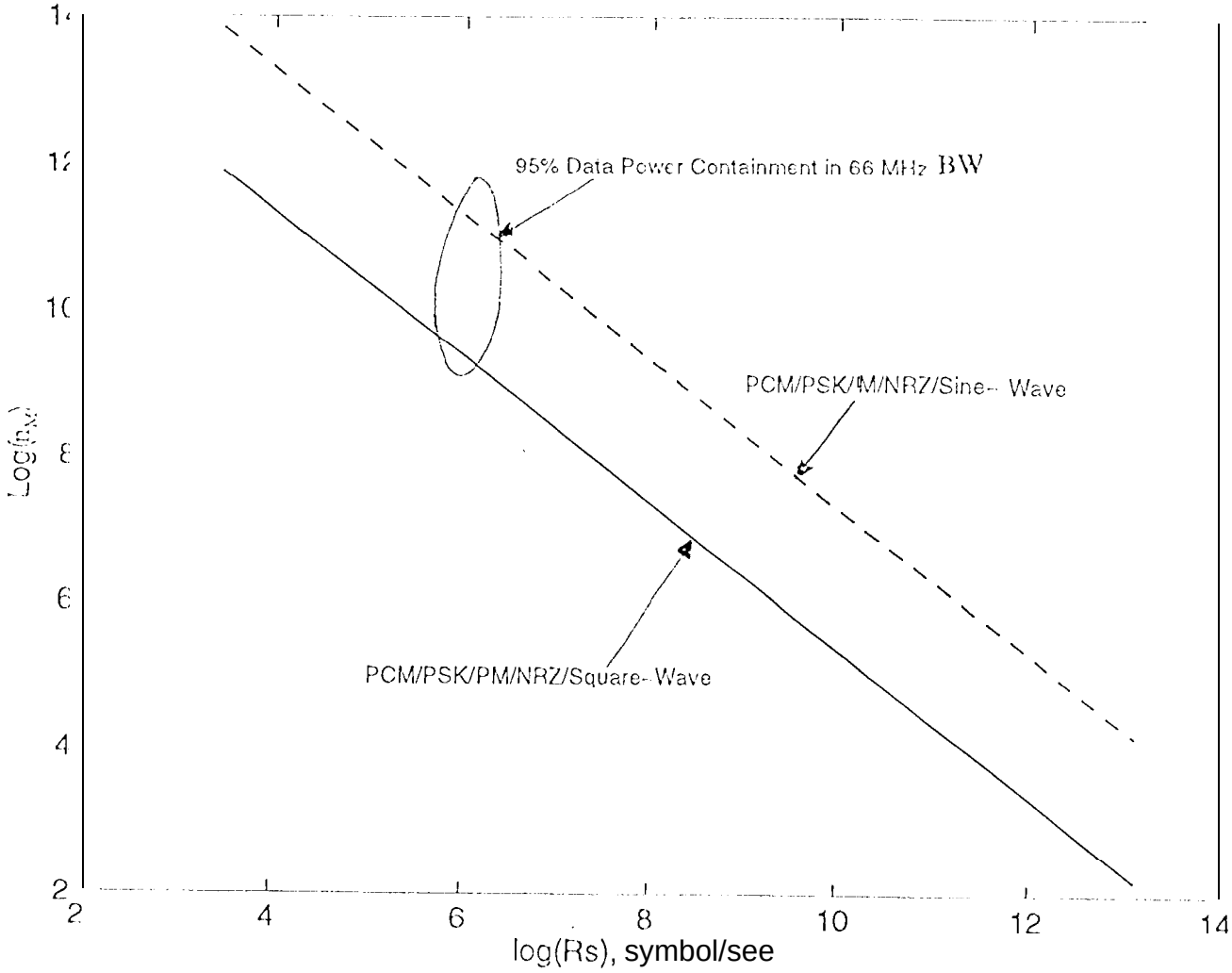

Figure 11. MAXIMUM SUB CARRIER FREQUENCY-TO-SYMBOL RATE RATIO AS A FUNTION OF SYMBOL RATE